HHS Public Access

Author manuscript

Nanotoxicology. Author manuscript; available in PMC 2019 January 08.

Published in final edited form as:

Nanotoxicology. 2017 August ; 11(6): 725–736. doi:10.1080/17435390.2017.1349200.

Evaluation of the molecular mechanisms associated with cytotoxicity and inflammation after pulmonary exposure to different metal-rich welding particles

Mohammad Shoeb, **Vamsi Kodali**, **Breanne Farris**, **Lindsey M. Bishop**, **Terence Meighan**, **Rebecca Salmen**, **Tracy Eye**, **Jenny R. Roberts**, **Patti Zeidler-Erdely**, **Aaron Erdely**, and **James M. Antonini**

Health Effects Laboratory Division, National Institute for Occupational Safety and Health, Morgantown, WV, USA

Abstract

Welding generates a complex aerosol of incidental nanoparticles and cytotoxic metals, such as chromium (Cr), manganese (Mn), nickel (Ni), and iron (Fe). The goal was to use both *in vivo* and *in vitro* methodologies to determine the mechanisms by which different welding fumes may damage the lungs. Sprague-Dawley rats were treated by intratracheal instillation (ITI) with 2.0 mg of gas metal arc-mild steel (GMA-MS) or manual metal arc-stainless steel (MMA-SS) fumes or saline (vehicle control). At 1, 3, and 10 days, bronchoalveolar lavage (BAL) was performed to measure lung toxicity. To assess molecular mechanisms of cytotoxicity, RAW264.7 cells were exposed to both welding fumes for 24 h (0–100 μg/ml). Fume composition was different: MMA-SS (41% Fe, 29% Cr, 17% Mn, 3% Ni) versus GMA-MS (85% Fe, 14% Mn). BAL indicators of lung injury and inflammation were increased by MMA-SS at all time points and by GMA-MS at 3 and 10 days after exposure. RAW264.7 cells exposed to MMA-SS had elevated generation of reactive oxygen species (ROS), protein-HNE (P-HNE) adduct formation, activation of ERK1/2, and expression of cyclooxygenase-2 (COX-2) compared to GMA-MS and control. Increased generation of ROS due to MMA-SS exposure was confirmed by increased expression of Nrf2 and heme oxygenase-1 (HO-1). Results of *in vitro* studies provide evidence that stainless steel welding fume mediate inflammatory responses via activation of ROS/P-HNE/ERK1/2/Nrf2 signaling pathways. These findings were corroborated by elevated expression of COX-2, Nrf2, and HO-1 in homogenized lung tissue collected 1 day after *in vivo* exposure.

Keywords

Welding; inflammation; cytotoxicity; reactive oxygen species; metals

CONTACT Mohammad Shoeb ywo7@cdc.gov Health Effects Laboratory Division, National Institute for Occupational Safety and Health, 1095 Willowdale Road (Mailstop 2015), Morgantown, WV 26505, USA.

Disclosure statement

The authors declare that they have no competing interests. The findings and conclusions in this report are those of the authors and do not necessarily represent the views of the National Institute for Occupational Safety and Health. Mention of brand name does not constitute product endorsement.

Introduction

According to the Bureau of Labor Statistics, ~397,900 workers were employed full-time as welders in USA in 2014 (Bureau of Labor Statistics, 2016). Importantly, many more workers worldwide, believed to exceed 5 million, perform welding as part of the job but are not classified as full-time welders. The health effects of welders have been difficult to study because of differences in workplace exposures, such as industrial setting, welding processes, materials and techniques used, duration of exposure, and ventilation (Antonini, 2014). Epidemiology indicates that welders may develop moderate to severe lung disease and other inflammatory pathologies, including occupational asthma, increased risk of respiratory infection due to immunosuppression, bronchitis, lung cancer, chemical pneumonitis, neurological deficits, and metal fume fever (Antonini, 2014).

Complex aerosols are generated during the welding process due to the consumption of a metal electrode or wire by extremely high temperatures (>2000 °C) formed by an arc at the weld area (Sferlazza & Beckett, 1991). Welding fumes are generally chain-like agglomerates of nanometer-sized primary particles with a mass median aerodynamic diameter of 0.2–0.5 μm (Antonini et al., 2011a; Jenkins et al., 2005; Zimmer & Biswas, 2001). The generated particles are a complex of potentially toxic metals that are dependent on the composition of the specific consumable wires/electrodes, and any fluxes or coatings on their surface or present in their core. Gas metal arc-mild steel (GMA-MS) welding and shielded, flux-coated manual metal arc-stainless steel (MMA-SS) welding are two common processes used by the welding industry. It has been observed that the particles formed from a flux-coated electrode (e.g., MMA-SS welding) are more water-solubility compared to GMA-MS welding, where fluxes are absent and the resulting particles are mostly insoluble (Taylor et al., 2003). GMA-MS welding fume is composed predominately of Fe with a small percentage of Mn present, whereas MMA-SS fume contain both Fe and Mn, but also contain significant amounts of Cr and Ni, two metals known to be cytotoxic and carcinogenic.

Previous toxicology studies indicate that pulmonary exposure to welding fumes can induce lung injury and inflammation (Antonini et al., 2007, 2010). MMA-SS fumes have been shown to generate ROS and be more cytotoxic and inflammatory in cellular and animal models compared to GMA-MS fumes (Antonini et al., 1996, 2005, 2011b; Leonard et al., 2010). This is likely due to the presence of metals such as Cr and Ni (Antonini et al., 2014; Badding et al., 2014). Also, particle reactivity and solubility appears to play a significant role in inflammation and toxicity associated with welding fume exposure (Taylor et al., 2003). As determined by microarray analysis, lung transcriptional effects in mice exposed to MMA-SS fume, but not GMA-MS fume, were associated with subchronic overexpression of inflammatory genes (Zeidler-Erdely et al., 2010). Also using similar methodologies, Oh et al. (2009, 2011) identified different genes that may be involved in lung cell inflammation, repair, and proliferation after inhalation exposure of rats to MMA-SS welding particles. However, specific molecular and cellular mechanisms related to the cytotoxic and inflammatory signaling and responses observed after welding fume exposure still are not well-defined.

Therefore, the primary objective of the current study was to investigate the molecular mechanisms associated with the cytotoxic and inflammatory responses after exposure to welding fume with different physical and chemical profiles to compare their potential in activating various inflammatory mediators using both a cellular and an animal model. To assess lung inflammation, male Sprague-Dawley rats were treated by intratracheal instillation (ITI) with GMA-MS or MMA-SS welding fumes, and bronchoalveolar lavage (BAL) was performed to assess lung toxicity and inflammation. To assess the molecular mechanisms associated with cytotoxicity caused by welding fumes, RAW264.7 macrophages were exposed to MMA-SS or GMA-MS welding fumes for different periods of time in a dose-dependent manner. Reactive oxygen species (ROS) generation and activation of different inflammatory mediators were determined.

Material and methods

Material

Dulbecco's modified Eagle's medium (DMEM) with 4 mM L-glutamine and 4.5 g/l glucose was purchased from Invitrogen Gibco (Grand Island, NY), phosphate-buffered saline (PBS) from Lonza (Walkersville, MD), fetal bovine serum (FBS) from Atlanta Biological (Norcross, GA). RIPA cell lysis buffer was purchased from Santa Cruz Biotechnology (Santa Cruz, CA). Dihydroethidium (DHE) fluorescent dye was purchased from Molecular Probes, Invitrogen (Carlsbad, CA). Mitochondrial membrane potential assay kit came from Cayman Chemical Company (Ann Arbor, MI). Alamar Blue was purchased from Invitrogen (Eugene, OR). Nuclear Extraction Kit (2900) from EMD Millipore (Billerica, MA), antibodies against ERK1/2, p-ERK1/2 (4695S and 9101S), Caspase-3/7 from Molecular Probes Inc. (C10423), GAPDH (2118S) were obtained from Cell Signaling Inc. (Beverly, MA); and antibodies against COX-2 (ab15191), protein-HNE (P-HNE) (ab46545), Nrf2 (ab89443), HO-1 (ab13248) and keap1 (ab66620) were obtained from Abcam Inc. (Cambridge, MA). Reagents and other chemicals used in Western blot analysis were obtained from Sigma-Aldrich (St. Louis, MO) and Biorad (Hercules, CA). All other reagents used were of analytical USP grade.

Welding fume characterization

The two welding fume samples were kindly generated and provided by Lincoln Electric Co. (Cleveland, OH). Bulk samples of the welding fumes were generated in an open front fume chamber (volume= 1 m^3) by a welder using an appropriate electrode and collected on 0.2 μm Nuclepore filters (Nuclepore Co., Pleasanton, CA). The welding samples were generated by: (i) GMA-MS E70S-3 electrode with argon and CO_2 as shielding gases and (ii) shielded manual metal arc welding with a stainless steel ER308-16-1 electrode (MMA-SS) as previously described (Antonini et al., 1999).

The aggregate size of the particles dispersed in water (hydrodynamic diameter, dH) was measured using dynamic light scattering (DLS) with a Malvern Zetasizer Nano-ZS instrument (Malvern Instruments Ltd., Worcestershire, UK). Particle stock was prepared by initially dispersing particles at 5 mg/ml concentration in 1 mg/ml bovine serum albumin (BSA). DLS measurements were performed in water, PBS, and DMEM (10% FBS) by

diluting the stock solution to 25 μg/ml. Table 1 shows average and standard deviation data from six independent samples.

Analysis of elements present in the welding samples was performed by inductively coupled plasma-atomic emission spectroscopy (ICP-AES) using NIOSH method 7303 modified for microwave digestion (NIOSH, 1994) as previously described (Antonini et al., 1999). In addition, portions of the different welding samples were suspended in distilled water, pH 7.4, and sonicated for 1 min with a Sonifier 450 Cell Disruptor (Branson Ultrasonics, Danbury, CT) to determine particle/metal solubility. The particle suspensions (total samples) were incubated for 24 h at 37 °C, and the samples were centrifuged at 12,000*g* for 30 min. The supernatants of the samples (soluble fraction) were recovered and filtered with a 0.22 μm filter (Millipore Corp., Bedford, MA). The pellets (insoluble fraction) were re-suspended in water. The sample suspensions (total, soluble, and insoluble fractions) were digested, and the metals analyzed by ICP-AES (NIOSH, 1994).

In vivo *toxicology studies*

Experimental design—Male Sprague-Dawley rats from Hilltop Lab Animals (Scottdale, PA), weighing 250–300 g and free of viral pathogens, parasites, mycoplasmas, Helicobacter, and CAR Bacillus, were used. The rats were acclimated for one week after arrival and were provided HEPA-filtered air, irradiated Teklad 2918 diet, and tap water *ad libitum*. All animal procedures used during the study were reviewed and approved by the National Institute for Occupational Safety and Health (NIOSH) Animal Care and Use Committee. The animal facilities are specific pathogen-free, environmentally controlled, and accredited by the Association for Assessment and Accreditation of Laboratory Animal Care International.

Welding fume exposure—The welding particle samples were suspended in sterile USP grade saline and sonicated to disperse the particulates. Rats (n = 4–6/group) were lightly anesthetized by an intraperitoneal injection of 0.6 ml (25 mg/kg body weight) of methohexital sodium for injection USP (Brevital 500 mg; JHP Pharmaceuticals, LLC, Rochester, MI) and treated by ITI with 2.0 mg/rat of GMA-MS or MMA-SS welding fumes in 300 μl of sterile USP-grade saline. Vehicle control animals were treated by ITI with 300 μl of sterile USP-grade saline. The dose was chosen based on results from a previous dose-response welding fume study (Antonini et al., 1996). It was found that an ITI welding particle dose of 0.2 mg/rat (regardless of fume type) induced no pulmonary response, whereas doses ≥5 mg/rat caused massive lung inflammation and prominent particle lung burden in all fumes studied. A goal of the current study was to choose a dose between the 0.2 and 5.0 mg/rat dose range used in the earlier study. In addition, the 2.0 mg/rat dose was determined to approximate an exposure of 52.1 days or ~10.4 weeks of exposure, based on 5-day work week (Antonini et al., 2014).

Bronchoalveolar lavage—At 1, 3, and 10 days after exposure by ITI, BAL was performed to assess lung injury and inflammation. Animals were euthanized with an overdose of a pentobarbital-based euthanasia solution (>100 mg/kg body weight, IP; Fatal-Plus Solution, Vortech Pharmaceutical, Inc., Dearborn, MI) and then exsanguinated by severing the abdominal aorta. The right lung was first lavaged with a 1 ml/100 g body

weight aliquot of calcium- and magnesium-free PBS, pH 7.4. The first fraction of recovered bronchoalveolar lavage fluid (BALF) was centrifuged at 500*g* for 10 min, and the resultant cell-free supernatant was analyzed for lactate dehydrogenase (LDH) as a marker for lung cell damage. LDH activity was determined by measuring the oxidation of lactate to pyruvate coupled with the formation of NADH at 340 nm. Measurements were taken with a COBAS MIRA auto-analyzer (Roche Diagnostic Systems, Montclair, NJ). The right lung was further lavaged with 6 ml aliquots of PBS until 30 ml were collected. These samples also were centrifuged for 10 min at 500*g* and the cell-free BALF discarded. The cell pellets from all washes for each rat were combined, washed, re-suspended in 1 ml of PBS buffer, counted, and differentiated.

Cellular evaluation—Total cell numbers recovered by BAL were determined using a Coulter Multisizer II and AccuComp software (Coulter Electronics, Hialeah, FL). Briefly, cell suspensions (5×10^4 cells) were spun using a Cytospin 3 centrifuge (Shandon Life Sciences International, Cheshire, UK) for 5 min at 800 rpm onto a slide. Cells (200/rat) were identified after labeling with Leukostat stain (Fisher Scientific, Pittsburgh, PA) as alveolar macrophages (AMs) and neutrophils (PMNs).

Preparation of rat lung tissue homogenates—To examine the effect of welding fume-induced expression of COX-2, Nrf2, HO-1 *in vivo*, left lung tissues were recovered from control and welding fume-exposed rats, separated, homogenized in PBS. Equal amount of proteins from homogenates were subjected to SDS–PAGE followed by western blot analysis as described in the following *in vitro* section.

In vitro *toxicology studies*

Cell culture—RAW264.7 mouse monocyte macrophages from American Type Culture Collection (Manassas, VA) were grown in DMEM containing 10% FBS, 1% penicillin/streptomycin in a 95% air 5% CO_2- humidified atmosphere at 37 °C. In all the studies, passages 11–15 were used.

Welding fume preparation—The welding particle samples were suspended in sterile USP-grade saline containing 1 mg/ml BSA and sonicated for 5 min to disperse the particulates.

Welding fume-induced toxicity assay—Approximately 1×10^5 RAW264.7 cells were seeded in a 96-well plate in complete DMEM media and incubated overnight in a 95% air and 5% CO_2-humidified atmosphere at 37 °C. Cells were treated with different concentrations of welding fumes (0, 3.125, 6.25, 12.5, 25, 50, and 100 μg/ml) for another 24 h, and cytotoxicity was assessed by the Alamar Blue assay. Briefly, resazurin, an active component of Alamar Blue reagent, which is nontoxic and non-fluorescent was added directly to each well, and the plates then were incubated at 37 °C for 1 h. Once resazurin enter the cells it is reduced to resorufin which is highly fluorescent and was measured excitation at 540–570 nm and emission at 580–610 nm.

Welding fume-induced ROS generation and change in mitochondrial membrane potential—Approximately 0.2×10^6 RAW264.7 macrophages were seeded in chamber slides in a complete DMEM media and incubated overnight in a 95% air and 5% CO_2-humidified atmosphere at 37 °C. Cells were treated with 6.25 μg/ml welding samples for 2 h. The cells were rinsed with PBS, incubated with DHE (2.5 μmol/L) or JC-1 dye at 37 °C for 10–15 min, fixed in 10% formalin. Cells were washed in PBS twice and mounted with ProLong Gold. Random images from each treatment group ($n = 4$) were taken using an Olympus AX70 upright microscope, and quantification was performed as previously described by Shoeb et al. (2017) using Olympus cell Sens Dimension 1.15 software (Olympus Corporation, Tokyo, Japan). Confocal microscopy was carried out using a Zeiss LSM 510 microscope equipped with an Argon laser and HeNe1 laser. Photomicroscopy of RAW264.7 macrophages was obtained using a 40 × objective.

Welding fume-induced P-HNE adducts formation and Nrf2 expression—Approximately 0.2×10^6 RAW264.7 macrophages were seeded in chamber slides in complete DMEM media and incubated overnight in a 95% air and 5% CO_2-humidified atmosphere at 37 °C. Cells were treated with 6.25 μg/ml welding fumes for 12 h. The cells were rinsed with PBS, fixed in 10% formalin for 15 min, rinsed with PBS, cells were blocked (2% BSA and 0.3% Triton-X) for 2–3 h and incubated with P-HNE and Nrf2 antibodies overnight. Next, cells were washed once with PBS and then incubated with fluorescent-tagged secondary antibodies for 45 min. Finally, the cells were washed in PBS twice and mounted with ProLong Gold. Random images from each treatment group ($n = 4$) were taken using an Olympus AX70 upright microscope, and quantification was performed as previously described by Shoeb et al. (2017) using Olympus cell Sens Dimension 1.15 software (Olympus Corporation, Tokyo, Japan).

mRNA analysis by qPCR—Gene expression for COX-2 and Hmox1 was determined by standard 96-well technology using the StepOne Plus (Applied Biosystems, Carlsbad, CA) with pre-designed Assays-on-Demand TaqMan probes and primers including COX-2 (Mm00478374_m1) and Hmox1 (Mm00446190_m1) (Applied Biosystems). Using 96-well plates, RNA (1 μg) was reverse transcribed using random hexamers (Applied Biosystems) and Superscript III (Invitrogen, Carlsbad, CA). cDNA was used for gene expression. Hypoxanthine-guanine phosphoribosyl-tranferase (HPRT) was used as the endogenous control.

Western blot analysis—The confluent RAW264.7 cells were incubated with or without welding fumes (6.25 and 18 μg/ml), in a 6-well plate for up to 24 h. The same experiment was performed on three separate days in duplicate from different stock of cells, using an experimental block design. The cells were washed with ice-cold PBS and lysed in ice-cold RIPA lysis buffer. The crude lysate was cleared by centrifugation at 12,000*g* for 10 min at 4 °C. Western blots were also performed using cytosolic nuclear extracts prepared from RAW264.7 cells pretreated with GMA-MS and MMA-SS (0–12 h) using Nuclear Extraction Kit 2900 (EMD Millipore, Billerica). An equal amount of macrophage cell lysate was separated using a 10–12% SDS–PAGE, and transferred to polyvinylidene difluoride membranes (Biorad, Hercules, CA). The membranes were incubated in blocking solution

containing 5% w/v dried fat-free milk and 0.1% v/v Tween-20 in Tris-buffered saline. Subsequently, the membranes were incubated with specific antibodies overnight. The blots were then washed, exposed to HRP-conjugated secondary antibodies for 1 h, and the antigen-antibody complex was detected by enhanced chemiluminescence (Pierce, Rockford, IL). The membranes were stripped and probed with antibodies against β-actin, glyceraldehyde-3-phosphate dehydrogenase (GAPDH) or proliferating cell nuclear antigen (PCNA) to ensure equal protein loading. Area under curve (AUC) was determined by ImageJ quantification of the represented blots.

Caspase-3/7 analysis—Activation of caspases-3/7 is an essential event in apoptosis process. In order to evaluate the level of apoptosis induced by GMA-MS and MMA-SS. Cells were treated with 6.25 μg/ml of either of the welding fume for 6 h and the induced caspase-3/7 was evaluated by treating the cells with 5 μM CellEvent Caspase-3/7 (Molecular Probes Inc., Catalog# C10423) substrate for 30 min. The level of caspase-3/7 was evaluated using flow cytometry with absorption/emission maxima of ~502/530 nm. The treatments were performed in triplicates and at least 5000 events were collected for each data point.

Statistical analysis—Results are mean ± standard error of measurement. Statistical analysis was performed using SigmaStat (Systat Software, Inc., SigmaPlot for Windows, San Jose, CA). The significance of difference between exposure groups within a time point for the *in vivo* study (Figures 2 and 3) was determined using a one-way analysis of variance (ANOVA) and the Tukey *post hoc* test, whereas other analyzes were performed using a Student's t-test. Densitometry was performed using ImageJ analysis software. The criterion of significance was set at $p < .05$.

Results

Welding fume characterization

The elemental composition and solubility of the two welding samples were quite different (Table 1). The GMA-MS sample was composed almost entirely of Fe (85%) and Mn (14%) and was relatively insoluble with a soluble-to-insoluble ratio of 0.020. The MMA-SS sample was composed of similar Mn levels but much less Fe as compared to the GMA-MS fume. Cr and Ni also were also present in the MMA-SS sample, but not in the GMA-MS sample. In addition, the MMA-SS sample was much more soluble with a soluble-to-insoluble ratio of 0.345. The majority of the soluble fraction of the MMA-SS fume was mostly Cr (87%) with some Mn (11%).

DLS measurement indicated GMA-MS welding particles agglomerated to a lesser extent than MMA-SS welding particles in solution with average dH of 246 and 549 nm, in water, respectively (Table 1). The agglomerates maintained or slightly decreased in size in cell culture media (DMEM containing 10% FBS). As expected the high salt concentration further enhanced the agglomerate sized in PBS. Particle morphology for the welding samples was different. The MMA-SS particles were both amorphous material (white structures in center of micrograph) and very fine, nanometer-size chain-like agglomerates (arrows; Figure 1(A)). The GMA-MS particles were agglomerates of submicron-sized

primary particles arranged as chain-like structures that were mostly spherical and more homogenous in size (Figure 1(B)).

Effect of in vivo welding fume exposure on lung injury and inflammation

To investigate *in vivo* pulmonary toxicity and inflammation, animals were treated with the different welding fumes or saline by ITI, and lung responses were measured at 1, 3, and 10 days after exposure. BALF LDH activity, an indicator of lung cell damage, was significantly elevated at all time points after exposure to MMA-SS compared to control (Figure 2). LDH was significantly elevated over control at 1 and 3 days after GMA-MS exposure, but returned to control levels by 10 days. In the assessment of *in vivo* lung inflammation, MMA-SS exposure significantly increased the number of PMNs recovered by BAL compared to control at all time points. In addition, MMA-SS increased BAL PMNs at Days 3 and 10 when compared with the GMA-MS group (Figure 3(A)). GMA-MS exposure significantly increased the number of PMNs at 1 and 3 days compared to control. No significant difference in the number of AMs recovered by BALF were observed between the GMA-MS and saline control groups (Figure 3(B)). MMA-SS exposure significantly increased AMs at 3 and 10 days compared to the other two groups.

Effect of welding fume-induced cell death in RAW264.7 macrophages

To investigate the concentration-dependent cytotoxic effect of different welding fumes, cell viability of RAW264.7 cells was determined. As shown in Figure 4, welding fume challenge caused an increase in cell death in a dose-dependent manner as measured at 24 h after exposure. However, a significant loss in viability was observed at a lower concentration of the MMA-SS sample (12.5 μg/ml) compared to the GMA-MS sample (25 μg/ml). Based on the results of the cell viability data, two concentrations were used to assess the mechanism of the RAW264.7 cells, taking into account for the different potencies of the two welding particle samples. Doses of 6.25 μg/ml (80% viable cells; MMA-SS) and 18 μg/ml (80% viable cells, GMA-MS) were used for the other analyzes.

Welding fume-induced ROS generation, P-HNE adduct formation and change in mitochondrial membrane potential in RAW264.7 macrophages

Because the welding fume samples caused RAW264.7 cell death, we next examined the *in vitro* generation of ROS as a possible mechanism. As observed by the amplified red fluorescence linked with DHE, the welding samples (6.25 μg/ml) induced ROS generation in macrophages at 2 h after exposure (Figure 5(A)). However, considerably less fluorescence linked with DHE was observed in macrophages exposed to GMA-MS fume compared to MMA-SS fume, suggesting a potential mechanism related to the difference observed in cytotoxicity (Figure 5(A)). Because increased ROS generation could result in the oxidation of polyunsaturated fatty acids (PUFAs) leading to the formation of various toxic lipid aldehydes, we next examined the effect of welding fume exposure on P-HNE adduct formation in RAW264.7 cells. As shown in Figure 5(B), exposure to the MMA-SS fume (6.25 μg/ml) caused increased PHNE adduct formation (green fluorescence) in the RAW264.7 cells at 12 h as compared to the GMA-MS fume and control at the non-cytotoxic dose used.

Furthermore, decreased mitochondrial membrane potential was observed in RAW264.7 macrophages treated with MMA-SS (6.25 μg/ml) for 2 h, as shown by the increase in JC1 staining measured as an increase in green fluorescence (Figure 5(C)). The control and GMA-MS groups did not cause much change in mitochondrial membrane potential at the non-cytotoxic dose (6.25 μg/ml) used as indicated by the absence of green fluorescence and presence of red fluorescence.

Welding fume-induced activation of caspase-3/7 in RAW264.7 macrophages

To investigate the potential molecular mechanism associated with welding fume-induced apoptosis in the RAW264.7 cells, we investigated the effect of MMA-SS and GMA-MS on caspase-3/7 activation *in vitro*. Caspases are family of cysteine proteases and are responsible for cellular apoptosis. Exposure of MMA-SS at a concentration of 6.25 μg/ml resulted in increased expression of caspase-3/7 compared to other groups (Figure 6).

Welding fume-induced activation of COX-2 in RAW264.7 macrophages

To further understand the mechanism and the potency of the two welding fumes, we exposed the RAW264.7 cells with two different concentrations (6.25 and 18 μg/ml) of the welding samples. We investigated the effect of welding fume-induced expression of COX-2 in RAW264.7 cells at the transcriptional and translational level for 24 h after exposure (Figure 7). Our results suggested that MMA-SS at a concentration of 6.25 μg/ml resulted in significantly increased expression of COX-2 compared to other groups. A similar response was observed when cells were treated with the higher 18 μg/ml dose (Figure 11(A)). MMA-SS exposure resulted in significant (~2.3 and 16-fold) increase in COX-2 protein expression, respectively (Figures 7(A,B) and 11(A)). Increased MMA-SS concentration caused a drastic increase in the potency of COX-2 expression as compared to GMA-MS in RAW264.7 cells. There was a 10-fold increase in COX-2 gene expression after MMA-SS exposure as compared control at the non-cytotoxic dose used.

Welding fume-induced phosphorylation of ERK1/2 MAP kinase in RAW264.7 macrophages

Because ERK1/2 is upstream of Nrf2 and its activation is required for Nrf2 nuclear translocation, we examined whether welding fume-challenged RAW264.7 cells activated the ERK1/2 MAP kinase signaling cascade (Figure 8). Exposure to 6.25 μg/ml of each welding fume caused phosphorylation of ERK1/2 MAP kinase. Expression of phosphorylated ERK1/2 MAP kinase was increased (~2-fold) after 5 min and (~6-fold) after 60 min of MMA-SS exposure compared to control (Figure 8). In addition, the expression of phosphorylated ERK1/2 MAP kinase of RAW264.7 cells was increased for up to 90 min following exposure to MMA-SS compared to control cells (Figure 8).

Welding fume-induced activation of Keap1-Nrf2 signaling pathway in RAW264.7 macrophages

Anti-inflammatory proteins, such as HO-1, provide protection against ROS-induced inflammatory signals. These proteins are regulated by Nrf2. Exposure to the MMA-SS fume (6.25 μg/ml) resulted in increased Nrf2 translocation (green fluorescence) in RAW264.7 cells at 12 h as compared to the GMA-MS fume and control (Figure 9(A)). We observed

decreased expression of Nrf2 in cytosolic fraction in time dependent manner (0–12 h), suggesting the translocation of Nrf2 to the nucleus (Figure 9(B)). To further examine the molecular mechanism and potency associated with these welding fume-induced lung inflammation and toxicity, the activation of Nrf2 and the expression of proteins and genes regulated by Nrf2 (e.g., HO-1) were examined in RAW264.7 cells at 24 h after exposure to 6.25 μg/ml and 18 μg/ml of MMA-SS and GMA-MS welding samples (Figures 10(A–D) and 11(A–D)). Exposure to MMA-SS (6.25 μg/ml) caused a significant increase (~2-fold) in the expression of Nrf2 (~95 kDa) protein and a significant increase in the expression of HO-1 (~32-fold) in whole cell lysate (Figure 10(A,C)). However, exposure to MMA-SS (18 μg/ml) caused a significant decrease (~8.5-fold) in the expression of Nrf2 protein and a significant increase in the expression of HO-1 (~2.5-fold) in whole cell lysate (Figure 11(A,D)), could be due to the rapid translocation of Nrf2 from cytosol to nucleus. Also, a significant increase (~4-fold) was observed in the level of HO-1 mRNA (Figure 10(D)), suggesting an overwhelming oxidative stress response from this exposure in RAW264.7 cells. However, no difference in expression of Keap1 protein was observed when comparing the two welding fumes at both concentrations with control (Figures 10(B) and11(C)).

Welding fume-induced expression of COX-2, Nrf2, and HO-1 in homogenized lung tissue

To corroborate the findings from the use of the RAW264.7 cells, expression of COX-2, Nrf2, and HO-1 were measured in homogenized lung tissue collected 1 day after ITI exposure to the welding fumes (Figure 12). In vivo exposure to MMA-SS caused a significant increase in the expression of COX-2 (~6-fold), Nrf2 (~2-fold), and HO-1 (~3-fold) in tissue compared lung to the other groups (Figure 12(A–C)).

Discussion

Inhalation of welding fumes is a common occupational exposure. Welding particles have unique physio-chemical properties. They are agglomerated chains of primary particles in the nanometer-size range composed of a complex mixture of different metals. Previous animal studies have indicated that metal composition (Antonini et al., 1996), particle size (Antonini et al., 2011a), and solubility (Taylor et al., 2003) of the welding particles greatly influence lung inflammation and injury. Stainless steel welding fumes are observed to be more cytotoxic and inflammatory in the lungs compared to mild steel fumes, likely due to the presence of Cr and Ni and increased cellular ROS production (Antonini et al., 2011b; Leonard et al., 2010). Microarray analysis studies have indicated that genes related to inflammation signaling and responses are overexpressed in lung tissue after exposure to stainless steel welding fumes (Oh et al., 2009; Oh et al., 2011; Zeidler-Erdely et al., 2010). However, specific details are lacking in regards to the molecular signaling mechanisms related to the inflammatory responses associated with welding fume exposure.

Two chemically distinct welding fumes were evaluated in the current study. The GMA-MS sample was relatively insoluble and composed of mostly Fe with some Mn, whereas the MMA-SS sample was more soluble and composed of both Fe and Mn but also contained significant amounts of Cr and Ni. *In vivo* pulmonary injury (BALF LDH activity) and inflammation (pulmonary influx of PMNs) were elevated at all time points and persisted for

10 days compared to control after ITI MMA-SS fume exposure. ITI GMA-MS fume exposure significantly increased injury and inflammation at early time points compared to control but had no effect at 10 days. In comparison of the two fumes, the MMA-SS sample was more pneumotoxic and inflammatory as evidenced by significant elevations in BALF LDH activity and influx of PMNs and AMs into the lungs at 3 and 10 days compared to the GMA-MS group. A possible mechanism by which stainless steel fumes may be more toxic than mild steel fumes may be related to the biopersistence of metals in the lungs after exposure. Previous animal studies have shown that the concentration of total metal in the lungs is significantly higher after exposure to stainless steel welding fumes compared to mild steel fumes (Antonini et al., 1996, 2010, 2011b).

The primary goal was to determine the mechanisms associated with these different pulmonary responses after exposure to the different welding fumes. Welding fumes contain transition metals and are known to undergo redox cycling subsequently leading to the generation of reactive ROS (Leonard et al., 2010; Taylor et al., 2003). Increased ROS generation could result in increased oxidation of PUFAs in the cell membrane which may cause lung injury, inflammation and cell death. Metal-rich welding particulates may induce numerous cytotoxic and inflammatory signals via activation of various kinases and transcription factors. To assess these potential mechanisms, RAW264.7 monocyte macrophages were exposed to MMA-SS or GMA-MS welding fumes for different periods of time in a dose-dependent manner. ROS generation and activation of different inflammatory mediators were determined.

Exposure of the RAW264.7 cells to the welding fume resulted in a dose-dependent increase in *in vitro* cytotoxicity. However, a significant loss in viability was observed at a lower concentration of the MMA-SS fume (12.5 μg/ml) compared to the GMA-MS fume (25 μg/ml). As evaluated by immunofluorescence, RAW264.7 cells treated with MMA-SS fume showed significantly higher production of ROS and P-HNE adduct formation as compared to GMA-MS exposed cells. It is likely the metal content of the welding fumes is mediating the generation of ROS in the cell membrane and potentially accelerating lipid peroxidation, resulting in the formation of toxic protein adducts. Due to its electrophilic properties, HNE can readily form adducts with proteins by modifying cysteine, histidine, or lysine residues (Jang et al., 2015). Several studies have reported the involvement of these adducts in numerous pathologies (Dalleau et al., 2013).

Further, we investigated the potential of these welding fumes in causing oxidative damage *in vitro*, possibly leading to apoptosis. In addition, mitochondrial membrane potential plays a vital role in maintaining cellular integrity (Chong & Maiese, 2004). Therefore, a possible change in mitochondrial membrane potential in RAW264.7 cells treated with welding fume may be indicative of oxidative stress. Our results showed that both welding fumes were capable of causing decreased mitochondrial membrane potential and increased expression of caspase-3/7, a marker of apoptosis. Importantly, MMA-SS was more potent, significantly decreasing mitochondrial membrane potential and increasing caspase-3/7 expression in RAW264.7 cells compared to other groups.

Metabolized products of COX-2 are crucial in protecting the body against infections but, overproduction of these products could results in acute or chronic inflammation (Bertolini et al., 2002). We investigated whether the expression and/or synthesis of COX-2 is affected by welding fume exposure *in vitro*. Our results demonstrated that exposure to both the welding fumes led to the elevated expression of COX-2. However, the expression and synthesis of COX-2 were significantly higher in MMA-SS-treated group.

Furthermore, it has been shown that P-HNE at micro-molar concentrations can lead to the phosphorylation and activation of various kinases and transcriptional factors (Chapple et al., 2013). Phosphorylation of kinases also may regulate Nrf2 activation and its accumulation and translocation to the nucleus (Bryan et al., 2013). Some of the major isoforms of kinases implicated in the regulation of inflammation are, ERK, p38, and JNK. ERK has been extensively studies for its involvement in proliferation and inflammation in variety of cells (Zipper & Mulcahy 2003). Our results indicated that exposure of RAW264.7 cells to the MMA-SS welding fumes resulted in the generation of ROS leading to the downstream phosphorylation of ERK1/2. Thus, our results support the hypothesis that stainless steel welding fume-induced P-HNE formation may enhance COX-2 production via the activation of ERK1/2 kinase pathways, leading to an inflammatory response.

Under normal conditions Nrf2 is linked to its endogenous inhibitor protein, Keap1 (Nrf2–Keap1 complex) in the cytoplasm. Numerous endogenous or environmental insults can dissociate this complex, leading to the accumulation and translocation of Nrf2 from the cytoplasm into the nucleus which in turn induces the transcription of HO-1 and other cytoprotective enzymes. As observed from our *in vitro* results, after 12 h, MMA-SS caused an increase in Nrf2 protein expression. Consistent with that finding, mRNA and protein for HO-1 increased after 24 h MMA-SS exposure. Together, these findings suggest that *in vitro* exposure to MMA-SS, possibly due to the presence of Cr and Ni, resulted in overwhelming generation of ROS in RAW264.7 cells and subsequent accumulation and translocation of Nrf2 from cytoplasm to nucleus resulting in the increased expression of HO-1 as compared to GMA-MS and control group.

Conclusion

In conclusion, the overall results of the *in vitro* RAW264.7 cell studies provide evidence that metal-rich welding particulates, specifically stainless steel welding fume, mediate inflammatory response via activation of ERK1/2/Nrf2/HO-1 signaling pathways. To determine the *in vivo* relevance of the *in vitro* findings in the RAW264.7 cells, expression of COX-2, Nrf2, and HO-1 were measured in homogenized lung tissue collected 1 day after ITI exposure to the welding fume (Figure 12). *In vivo* exposure to MMA-SS fume caused a significant increase in the expression of COX-2, Nrf2, and HO-1 in lung tissue compared to the GMA-MS fume and the saline control. We propose one of the possible mechanism presented in Figure 13 as to how stainless steel welding particles may induce lung injury and inflammation. A previous study indicates that hexavalent Cr, Ni, and Mn alone or in combination affect cell signaling of human lung epithelial cells *in vitro* by influencing the interplay between stress-response signaling (e.g., p38, SAPK/JNK) and anti-apoptotic signaling (ERK1/2) molecules (Tessier & Pascal, 2006). Studies are ongoing in our

laboratory attempting to determine if the responses of the two welding fumes used in the current study are due to differences in metal composition by examining which metal or metals associated with the welding fumes may be responsible for the responses observed.

Acknowledgments

The authors thank Dr. Stephen Leonard for critical review of the article.

Funding

This study was supported by funding from NIOSH project # 927ZLEG.

References

Antonini JM. 2014 Health effects associated with welding In: Bassim N, editor. Comprehensive Materials Processing. Chapter 8. Oxford, UK: Elsevier Ltd; 49–70.

Antonini JM, Badding MA, Meighan TG, Keane MK, Leonard SS, Roberts JR. 2014 Evaluation of the pulmonary toxicity of a fume generated from a nickel-, copper-based electrode to be used as a substitute in stainless steel welding. Environ Health Insights 8(Suppl 1):11–20. [PubMed: 25392698]

Antonini JM, Keane M, Chen BT, Stone S, Roberts JR, Schwegler-Berry D, et al. 2011a Alterations in welding process voltage affect the generation of ultrafine particles, fume composition, and pulmonary toxicity. Nanotoxicology 5:700–10. [PubMed: 21281223]

Antonini JM, Krishna Murthy GG, Rogers RA, Albert R, Ulrich GD, Brain JD. 1996 Pneumotoxicity and pulmonary clearance of different welding fume particles after intratracheal instillation in the rat. Toxicol Appl Pharmacol 40:188–99.

Antonini JM, Lawryk NJ, Krishna Murthy GG, Brain JD. 1999 Effect of welding fume solubility on lung macrophage viability and function *in vitro*. J Toxicol Environ Health Part A 58:343–63. [PubMed: 10580758]

Antonini JM, Leonard SS, Roberts JR, Solano-Lopez C, Young S-H, Shi X, Taylor MD. 2005 Effect of stainless steel manual metal arc welding fume on free radical production, DNA damage, and apoptosis induction. Mol Cell Biochem 279:17–23. [PubMed: 16283511]

Antonini JM, Roberts JR, Chapman R, Soukup JM, Ghio AJ, Sriram K. 2010 Pulmonary toxicity and extrapulmonary tissue distribution of metals after repeated exposure to different welding fumes. Inhal Toxicol 22:805–16. [PubMed: 20560776]

Antonini JM, Roberts JR, Stone S, Chen BT, Schwegler-Berry D, Chapman R, et al. 2011b Persistence of deposited metals in the lungs after stainless steel and mild steel welding fume inhalation in rats. Arch Toxicol 85:487–98. [PubMed: 20924559]

Antonini JM, Stone S, Roberts JR, Chen B, Schwegler-Berry D, Afshari AA, Frazer DG. 2007 Effect of short-term stainless steel welding fume inhalation exposure on lung inflammation, injury, and defense responses in rats. Toxicol Appl Pharmacol 223:234–45. [PubMed: 17706736]

Badding MA, Fix NR, Antonini JM, Leonard SS. 2014 A comparison of cytotoxicity and oxidative stress from welding fumes generated with a new nickel-, copper-based consumable versus mild and stainless steel-based welding in RAW 264.7 mouse macrophages. PLoS One 6:e101310.

Bertolini A, Ottani A, Sandrini M. 2002 Selective COX-2 inhibitors and dual acting anti-inflammatory drugs: critical remarks. Curr Med Chem 9:1033–43. [PubMed: 12733982]

Bryan HK, Olayanju A, Goldring CE, Park BK. 2013 The Nrf2 cell defence pathway: Keap1-dependent and -independent mechanisms of regulation. Biochem Pharmacol 85:705–17. [PubMed: 23219527]

Bureau of Labor Statistics. 2016 Occupational outlook handbook employment: welders, cutter, solders, and brazers. [Online] US Department of Labor Available at: http://www.bls.gov/ooh. Accessed on 12 January 2016.

Chapple SJ, Cheng X, Mann GE. 2013 Effects of 4-hydroxynonenal on vascular endothelial and smooth muscle cell redox signaling and function in health and disease. Redox Biol 23:319–31.

Chong ZZ1, Maiese K. 2004 Targeting WNT, protein kinase B, and mitochondrial membrane integrity to foster cellular survival in the nervous system. Histol Histopathol 19:495–504. [PubMed: 15024710]

Dalleau S, Baradat M, Guéraud F, Huc L. 2013 Cell death and diseases related to oxidative stress: 4-hydroxynonenal (HNE) in the balance. Cell Death Differ 20:1615–30. [PubMed: 24096871]

Leonard SS, Chen BT, Stone SG, Schwegler-Berry D, Kenyon AJ, Frazer DG, Antonini JM. 2010 Comparison of stainless and mild steel welding fumes in generation of reactive oxygen species. Part Fibre Toxicol 7:32. [PubMed: 21047424]

Jang EJ, Jeong HO, Park D, Kim DH, Choi YJ, Chung KW, et al. 2015 Src tyrosine kinase activation by 4-hydroxynonenal upregulates p38, ERK/AP-1 signaling and COX-2 expression in YPEN-1 cells. PLoS ONE 14:10.

Jenkins NT, Pierce WM-G, Eagar TW. 2005 Particle size distribution of gas metal and flux cored arc welding fumes. Welding J 84:156s–63s.

National Institute for Occupational Safety and Health (NIOSH). 1994 Elements by ICP (hot block/HCl/HNO3 digestion): method 7303 NIOSH Manual of Analytical Methods, 4th ed. Washington, DC: U.S. Department of Health and Human Services Publication No. 98–119.

Oh J-H, Yang M-J, Heo J-D, Yang Y-S, Park H-J, Park S-M, et al. 2011 Inflammatory response in rat lungs with recurrent exposure to welding fumes: a transcriptomic approach. Toxicol Ind Health 28:203–15. [PubMed: 21730038]

Oh J-H, Yang M-J, Yang Y-S, Park H-J, Heo SH, Lee E-H, et al. 2009 Microarray-based analysis of the lung recovery process after stainless-steel welding fume exposure in Sprague-Dawley rats. Inhal Toxicol 21:347–73. [PubMed: 19235613]

Sferlazza SJ, Beckett WS. 1991 The respiratory health of welders. Am Rev Respir Dis 143:1134–48. [PubMed: 2024826]

Shoeb M, Kodali V, Farris B, Bishop L, Meighan T, Salmen R, et al. 2017 Oxidative stress, DNA methylation, and telomere Length Changes in Peripheral Blood Mononuclear Cells after Pulmonary Exposure to Metal-Rich Welding Nanoparticles. Nanoimpact 5:61–9.

Taylor MD, Roberts JR, Leonard SS, Shi X, Antonini JM. 2003 Effects of welding fumes of differing composition and solubility on free radical production and acute lung injury and inflammation in rats. Toxicol Sci 75:181–91. [PubMed: 12832661]

Tessier DM, Pascal LE. 2006 Activation of MAP kinases by hexavalent chromium, manganese and nickel in human lung epithelial cells. Toxicol Lett 167:114–21. [PubMed: 17045426]

Zeidler-Erdely PC, Li S, Kashon ML, Antonini JM. 2010 Response of the mouse lung transcriptome to welding fume: effects of stainless and mild steel fumes on lung gene expression in A/J and C57BL/6J mice. Respir Res 11:70 [PubMed: 20525249]

Zimmer AT, Biswas P. 2001 Characterization of the aerosols resulting from arc welding processes. J Aerosol Sci 32:993–1008.

Zipper LM, Mulcahy RT. 2003 Erk activation is required for Nrf2 nuclear localization during pyrrolidine dithiocarbamate induction of glutamate cysteine ligase modulatory gene expression in HepG2 cells. Toxicol Sci 73:124–34. [PubMed: 12657749]

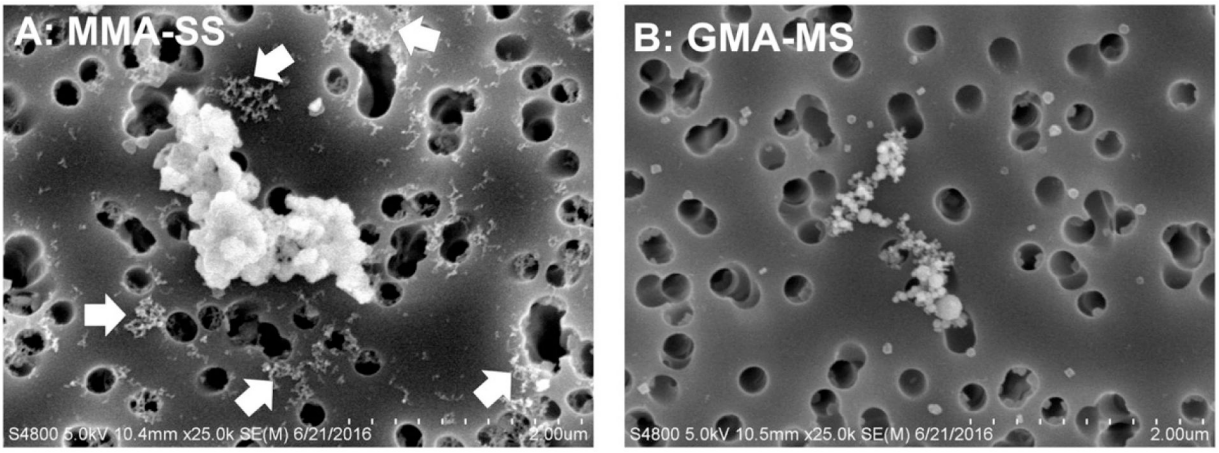

Figure 1.

Representative scanning electron micrographs of (A) MMA-SS and (B) GMA-MS welding particles dispersed onto filters; arrows indicate small, very fine chain-like agglomerates in (A). Dashed micron bar equals 2 μm.

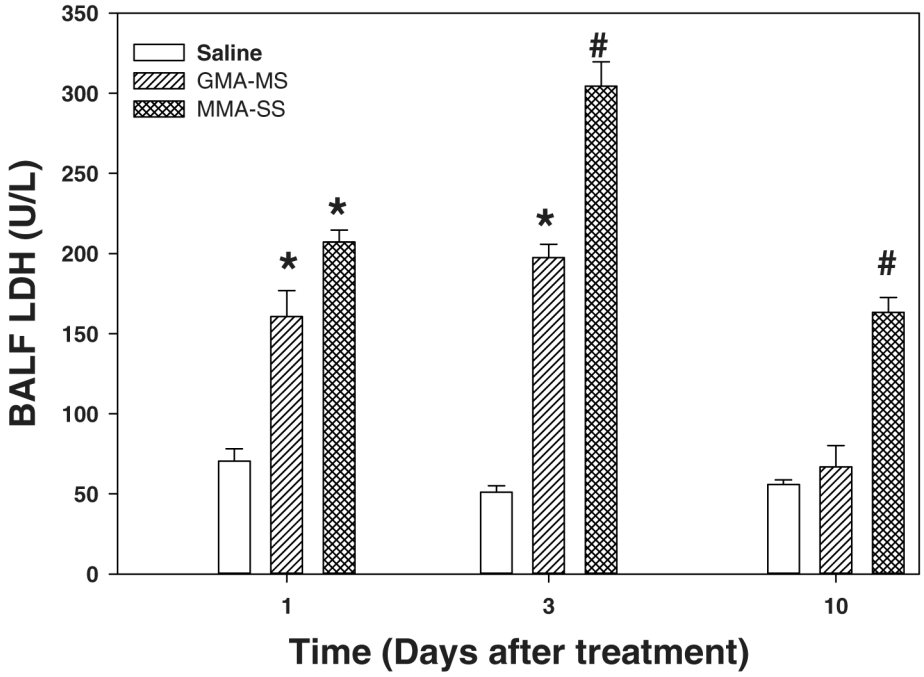

Figure 2.

LDH activity in acellular BALF at 1, 3, and 10 days after ITI exposure to 2.0 mg/rat of MMA-SS or GMA-MS welding fumes. Vehicle controls were received saline by ITI. (n = 4–6; values are mean ± standard error; *Significantly different from saline control, $p < .05$; #significantly different from saline control and GMA-MS groups).

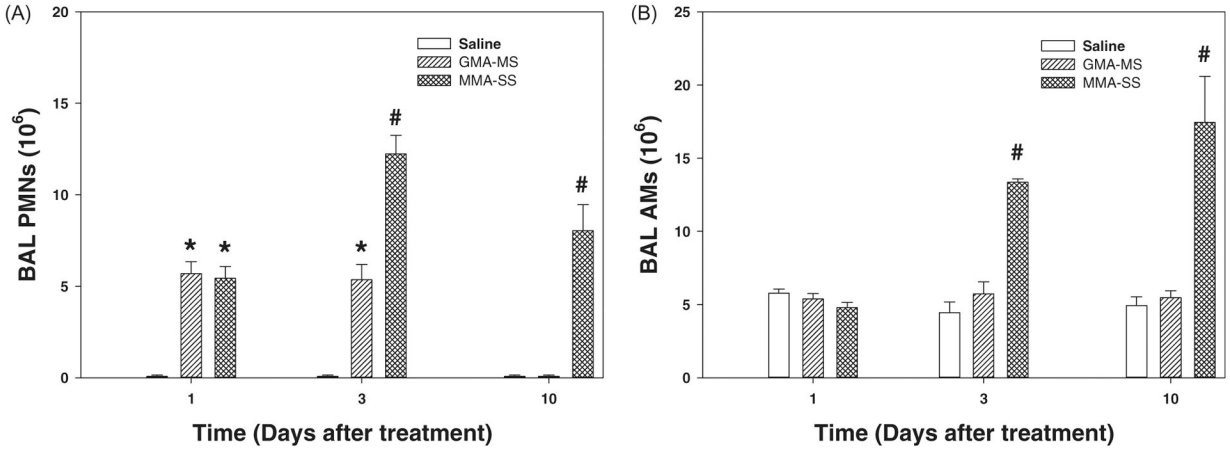

Figure 3.

(A) PMNs and (B) AMs recovered by BAL at 1, 3, and 10 days after ITI exposure to 2.0 mg/rat of MMA-SS or GMA-MS welding fumes. Vehicle controls received saline by ITI (n = 4–6; values are mean ± standard error; *Significantly different from saline control, $p < .05$; #significantly different from saline control and GMA-MS groups).

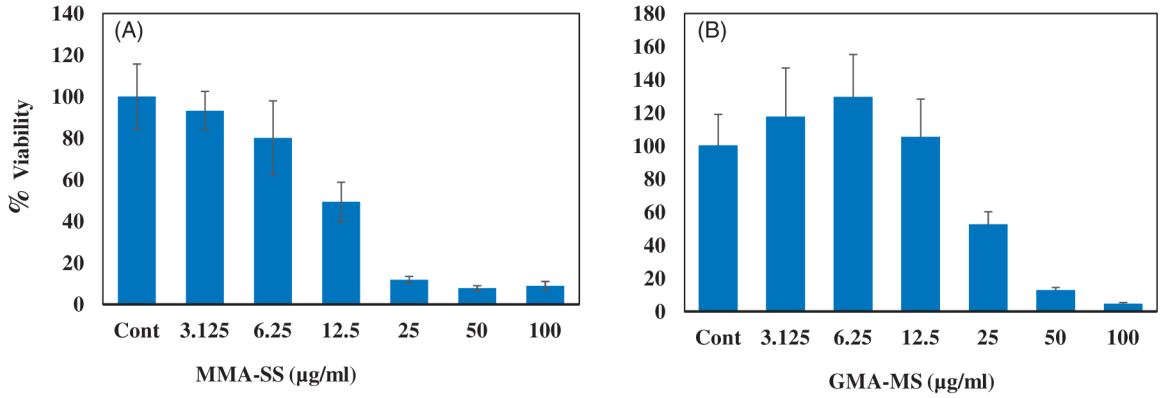

Figure 4.

RAW264.7 cell viability at 24 h after addition of different concentrations of (A) MMA-SS or (B) GMA-MS welding fumes. Vehicle control (Cont) cells received saline. Cell viability was determined by measuring percent cell death after welding fume exposure compared to saline controls ($n = 6$; values are mean ± standard error).

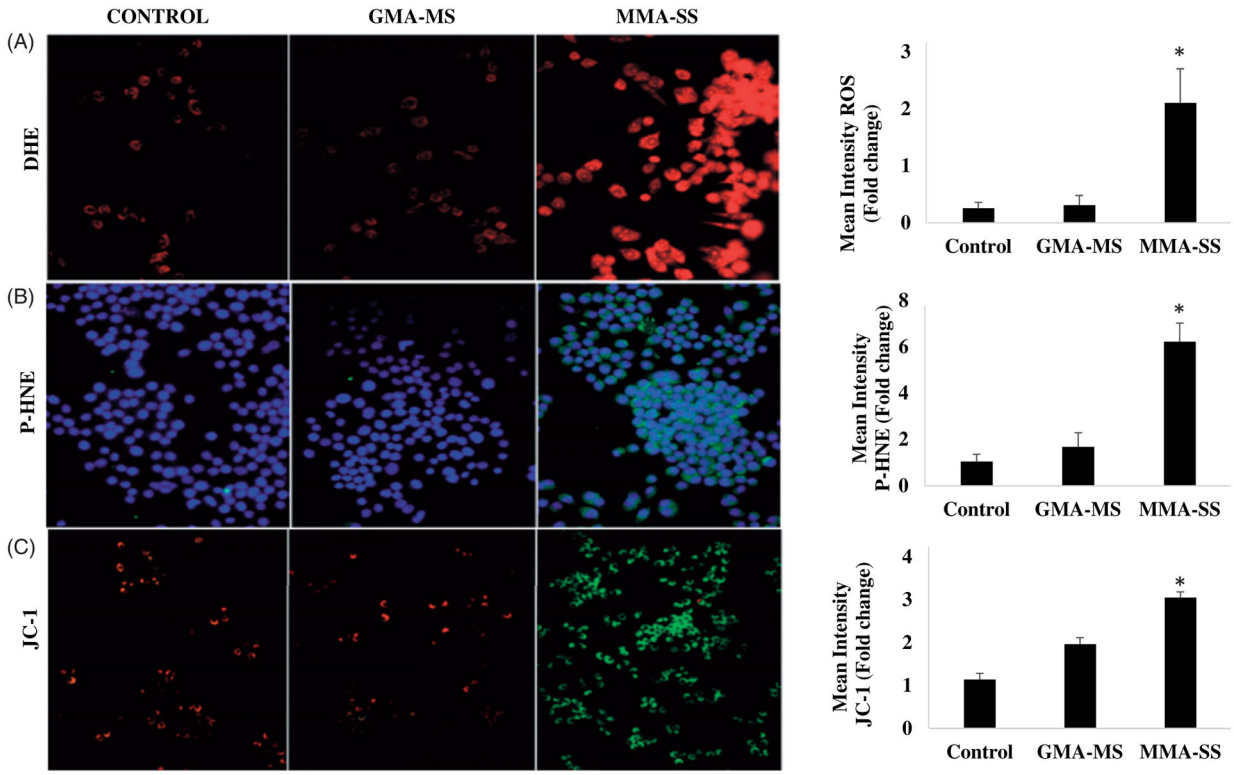

Figure 5.

(A) RAW264.7 cell ROS generation (DHE red fluorescence) and mean fluorescence intensity at 2 h after treatment with 6.25 μg/ml of MMA-SS or GMA-MS welding fumes; (B) RAW264.7 cell P-HNE adduct formation (green fluorescence) and mean fluorescence intensity at 12 h after treatment with 6.25 μg/ml of MMA-SS and GMA-MS welding fumes; (C) change in mitochondrial membrane potential (green fluorescence; 20× objective) and mean fluorescence intensity at 2 h after treatment with 6.25 μg/ml of MMA-SS or GMA-MS welding fumes. Vehicle control cells received saline.

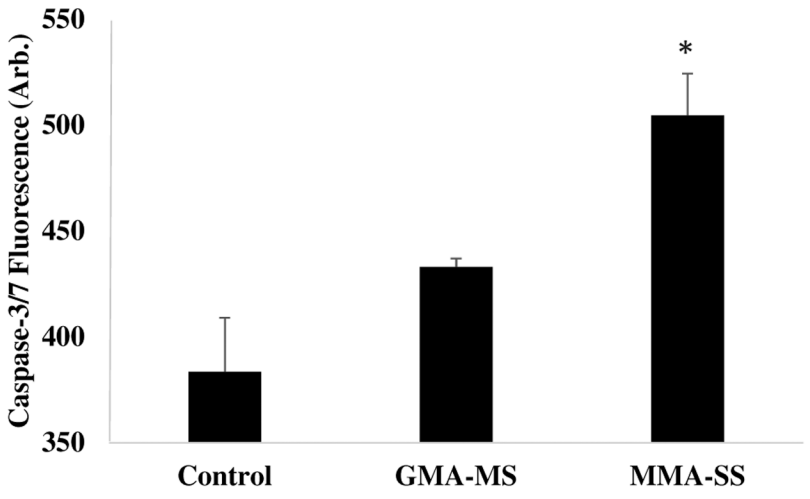

Figure 6.

In *vitro* expression of Caspase-3/7 in RAW264.7 cells at 6 h after treatment with 6.25 μg/ml of MMA-SS or GMA-MS welding fumes. Vehicle control cells received saline ($n = 3$; values are mean ± standard error).

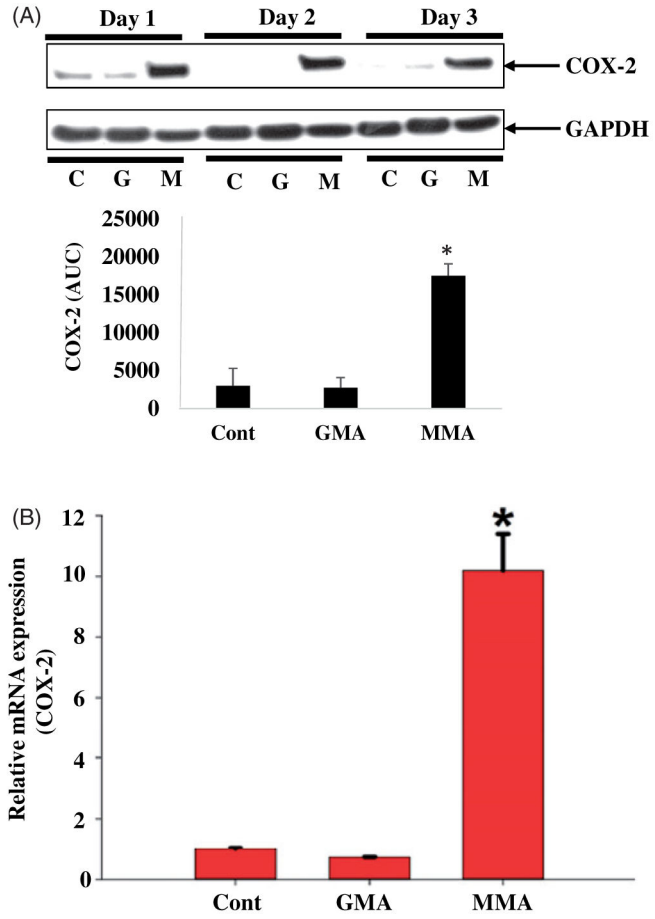

Figure 7.

(A) Representative western blot and densitometer measurement of *in vitro* protein expression of COX-2 in RAW264.7 cells at 24 h after treatment with 6.25 μg/ml of MMA-SS (M) or GMA-MS (G) welding fumes. Vehicle control cells received saline. (B) *In vitro* COX-2 expression in RAW264.7 cells at 24 h after treatment with 6.25 μg/ml of MMA-SS or GMA-MS welding fumes ($n = 3$; values are mean ± standard error; *significantly different from other groups, $p < .05$).

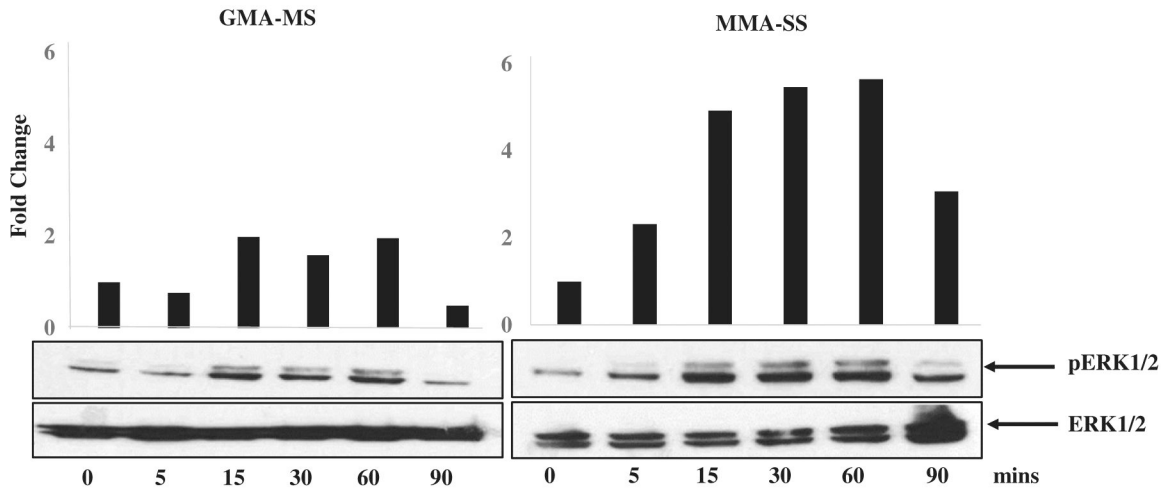

Figure 8.

Representative Western blot of *in vitro* protein expression of ERK1/2 MAP kinase and phosphorylated ERK1/2 MAP kinase (pERK1/2) and densitometer measurement of pERK1/2 in RAW264.7 cells at 0–90 min after treatment with 6.25 μg/ml of MMA-SS or GMA-MS welding fumes. Vehicle control cells received saline.

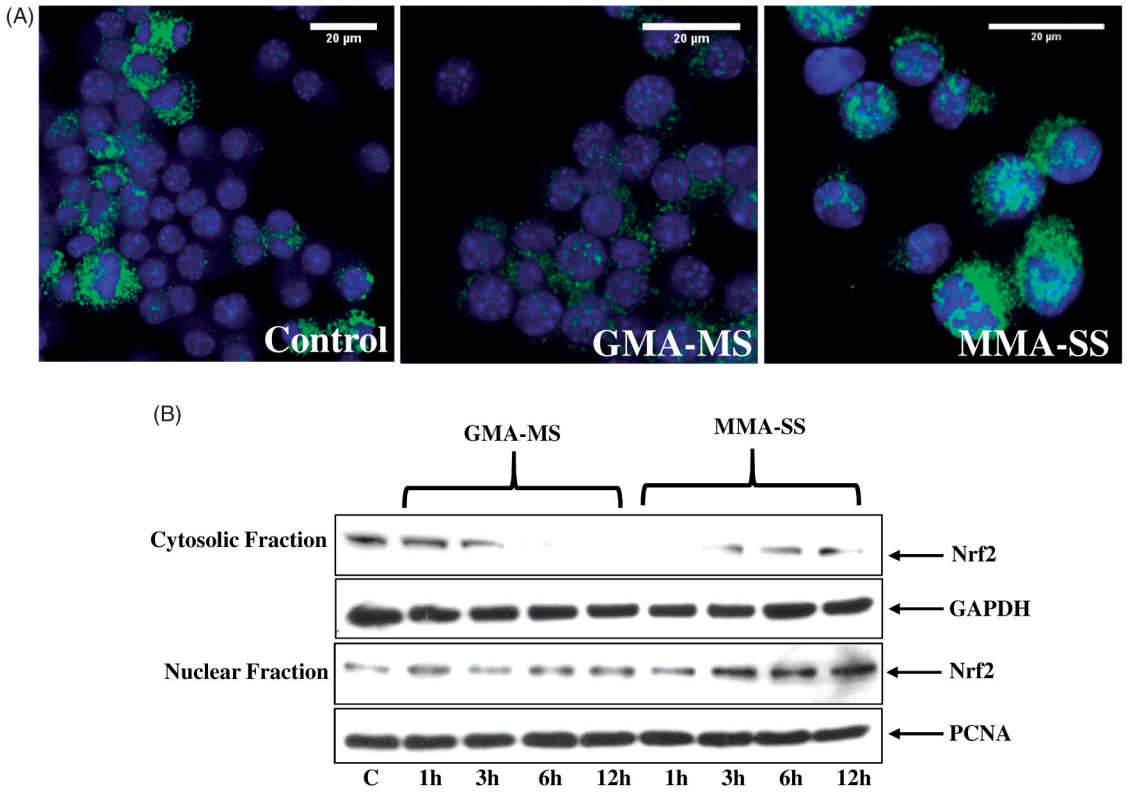

Figure 9.

(A) *In vitro* translocation of Nrf2 in RAW264.7 cells (green fluorescence) at 12 h after treatment with saline or 6.25 μg/ml of MMA-SS or GMA-MS welding fumes. (B) Representative Western blot measurement of cytosolic and nuclear extracts *in vitro* protein expression of Nrf2, at 0–12 h after treatment with 6.25 μg/ml of MMA-SS or GMA-MS welding fumes. Vehicle control cells received saline ($n = 3$).

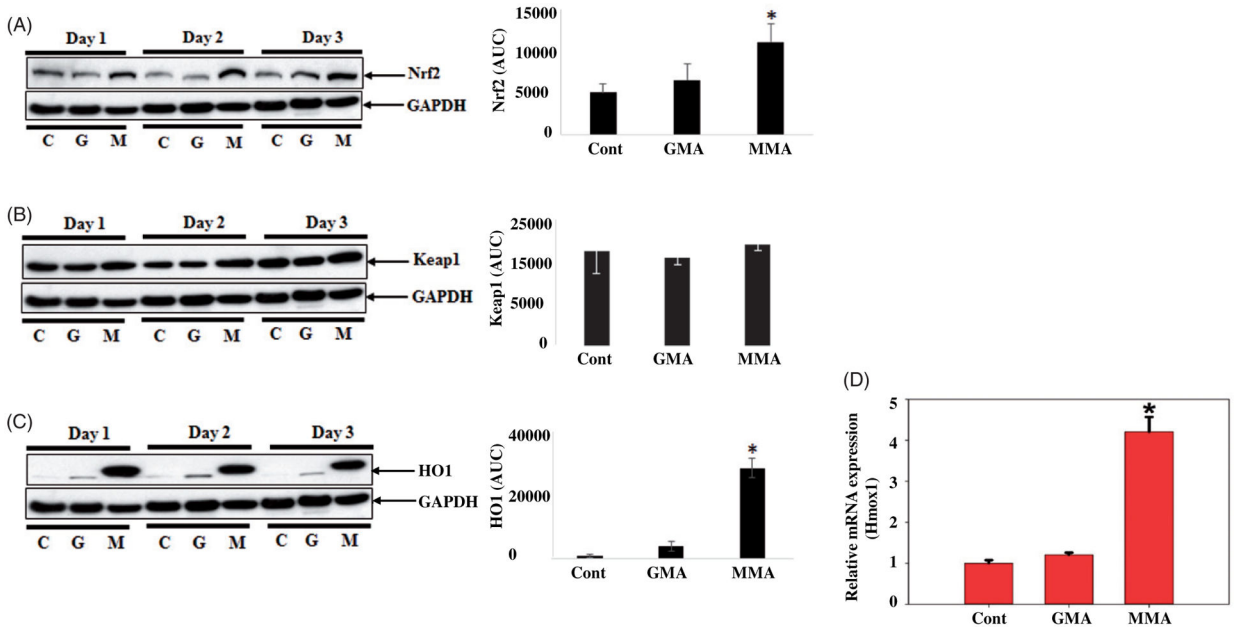

Figure 10.

Representative western blot and densitometer measurements of *in vitro* protein expression of (A) Nrf2, (B) Keap1, and (C) HO-1 in RAW264.7 cells at 24 h after treatment with 6.25 μg/ml of MMA-SS (M) or GMA-MS (G) welding fumes. (D) *In vitro* Hmox-1 gene expression in RAW264.7 cells at 24 h after treatment with 6.25 μg/ml of MMA-SS or GMA-MS welding fumes. Vehicle control cells received saline ($n = 3$).

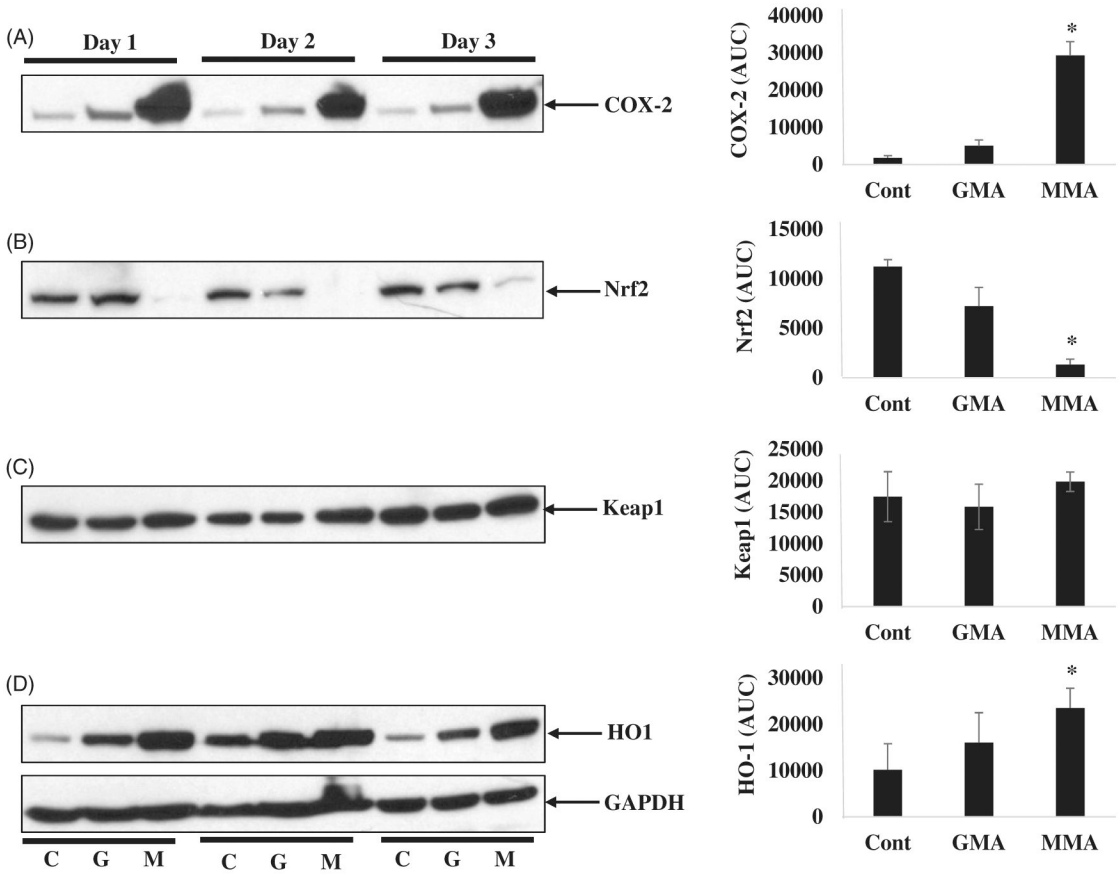

Figure 11.

Representative Western blot and densitometer measurements of *in vitro* protein expression of (A) COX-2, (B) Nrf2, (C) Keap1, and (D) HO-1 in RAW264.7 cells at 24 h after treatment with 18 μg/ml of MMA-SS (M) or GMA-MS (G) welding fumes. Vehicle control cells received saline ($n = 3$; values are mean ± standard error; *significantly different from other groups, $p < .05$).

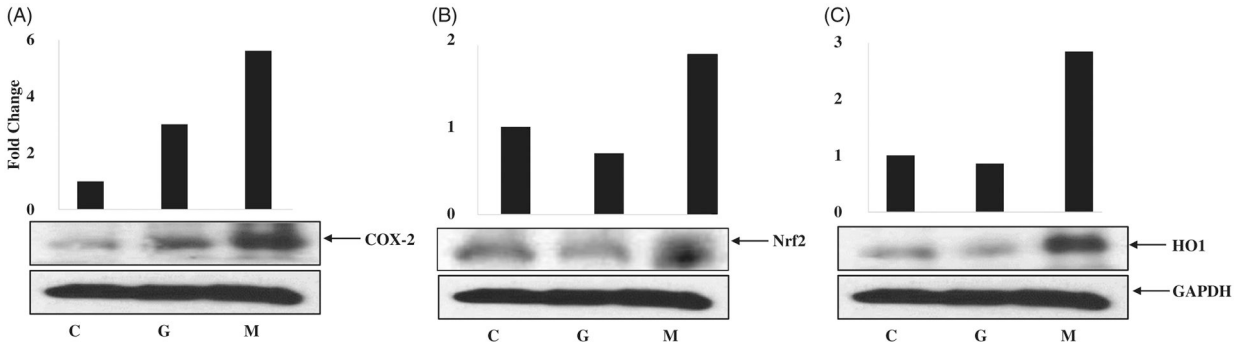

Figure 12.

Representative western blot and densitometer measurements of *in vivo* protein expression of (A) COX-2, (B) Nrf2, and (C) HO-1 in homogenized lung tissue at 1 day after ITI exposure to 2.0 mg/rat of MMA-SS (M) or GMA-MS (G) welding fumes. Vehicle controls received normal saline by ITI.

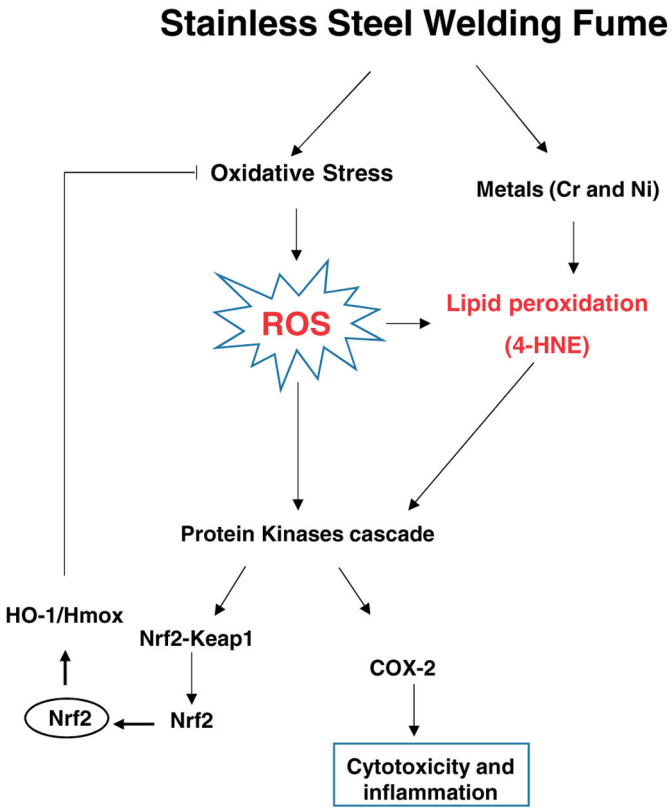

Figure 13.

Schematic diagram depicting proposed mechanism by which stainless steel welding fume induces cytotoxicity by ROS generation and activation of inflammatory mediators. Pathway illustrates how welding particles (directly) and/or its metal content could phosphorylate ERK1/2 kinase via ROS generation which in turn activate the formation of inflammatory marker and the translocation of Nrf2 in the nucleus.

Table 1.

Welding particle characterization.

Sample	Metal composition (weight %)[a]	Soluble/insoluble ratio	Water (*Z*-average; d.nm)[b]	PBS (*Z*-average; d.nm)[b]	DMEM (10% FBS) (*Z*-average; d.nm)[b]
GMA-MS: gas metal arc mild steel	85% Fe 14% Mn	0.020	246 ± 3	913 ± 101	283 ± 7
MMA-SS: manual metal arc: stainless steel	41% Fe 28% Cr 17% Mn 3% Ni	0.345 (87% Cr, 11% Mn)	549 ± 19	710 ± 48	459 ± 37

[a]Relative to all metals analyzed.

[b]Measurements were performed at particle concentration of 25 μg/ml. Data represents average plus standard deviations from six independent samples (d.nm = hydrodynamic diameter in nanometers).